Atmospheric Environment 42 (2008) 8470–8483

Contents lists available at ScienceDirect

Atmospheric Environment

journal homepage: www.elsevier.com/locate/atmosenv

Global model simulation of summertime U.S. ozone diurnal cycle and its sensitivity to PBL mixing, spatial resolution, and emissions

Jin-Tai Lin [a,1], Daeok Youn [c], Xin-Zhong Liang [b], Donald J. Wuebbles [a,*]

[a] Department of Atmospheric Sciences, University of Illinois at Urbana-Champaign, 105 S. Gregory Street, Urbana, IL 61801, USA
[b] Illinois State Water Survey, University of Illinois at Urbana-Champaign, 2204 Griffith Drive, Champaign, IL 61820-7495, USA
[c] Research Institute of Basic Sciences and School of Earth and Environmental Sciences, Seoul National University, Sillim 9-dong, Gwanak-gu, Seoul 151-747, South Korea

ARTICLE INFO

Article history:
Received 9 January 2008
Received in revised form 7 August 2008
Accepted 8 August 2008

Keywords:
Ozone diurnal cycle
PBL mixing
Resolution
Emissions

ABSTRACT

Simulation of summertime U.S. surface ozone diurnal cycle is influenced by the model representation of planetary boundary layer (PBL) mixing, spatial resolution, and precursor emissions. These factors are investigated here for five major regions (Northeast, Midwest, Southeast, California, and Southwest) by using the Model for Ozone And Related chemical Tracers version 2.4 (MOZART-2.4), with important modifications, to conduct sensitivity experiments for summer 1999 with three PBL mixing schemes, two horizontal resolutions and two emissions datasets. Among these factors, the PBL mixing is dominant. The default non-local scheme well reproduces the observed ozone diurnal variation, where the timing for the afternoon maximum and the morning minimum is within 1 h of the observed; biases for the minimum are less than 5 ppb except over the Southeast; and the ozone maximum–minimum contrast (OMMC) is within 10 ppb of observations except for the overprediction by 18.9 ppb over the Northeast. In contrast, the local scheme significantly overestimates the OMMC by 10–34 ppb over all regions as ozone and precursors are trapped too close to the ground. On the other hand, the full-mixing assumption underestimates the OMMC by 0–25 ppb, except over the Northeast, as the nighttime ozone decline is greatly underpredicted. As compared to PBL mixing, the effects of horizontal resolutions and precursor emissions being used are smaller but non-negligible. Overall, with the non-local mixing scheme, relatively high horizontal resolution ($\sim 1.1^{\circ}$) and updated emissions data, the modified MOZART is capable of simulating the main features of the observed ozone diurnal cycle.

1. Introduction

Over much of the U.S. surface ozone (i.e., ozone in the near surface air) undergoes significant diurnal variation in summer due to interactions and changes in major determinants including precursor emissions, solar radiation, dry deposition, titration by nitrogen oxides (NO_x) (Sillman, 1999), and vertical mixing in the planetary boundary layer (PBL), as well as mixing with the free troposphere (Zhang et al., 2006a; Huang et al., 2007). In particular, the vertical mixing plays an important role in redistributing ozone concentrations in the PBL. During the daytime, ozone is produced near the surface with the maximum in the afternoon through precursor reactions in the presence of strong solar radiation; meanwhile the PBL is typically unstable and thus surface ozone is transported efficiently upward into the upper PBL. During the

* Corresponding author. Tel.: +1 217 2441568; fax: +1 217 2444393.
E-mail addresses: jlin5@atmos.uiuc.edu (J.-T. Lin), ydo88@atmos.uiuc.edu (D. Youn), xliang@uiuc.edu (X.-Z. Liang), wuebbles@atmos.uiuc.edu (D.J. Wuebbles).
[1] Present address: School of Engineering and Applied Sciences, Harvard University, 19 Oxford Street, Cambridge, MA 02138, USA.

1352-2310/$ – see front matter © 2008 Elsevier Ltd. All rights reserved.
doi:10.1016/j.atmosenv.2008.08.012

nighttime, the PBL is stable with weak vertical mixing of pollutants; and surface ozone decreases to the minimum level around sunrise due to destruction processes like dry deposition and NO_x titration. The observed maximum level of ozone in the afternoon is normally several times larger than the minimum in the early morning (http://www.epa.gov/ttn/airs/airsaqs/detaildata/downloadaqsdata.htm). It is important to simulate this diurnal pattern and assess the roles of different atmospheric processes in maintaining such pattern. Meanwhile the diurnal variation of surface ozone provides a useful ways to evaluate the model capability and deficiency throughout the day. It also aids in evaluating the modeling uncertainties in various applications such as projecting climate change effects on pollution levels, estimating long-range transport effects on domestic air quality, and estimating the pollution mitigation efficiency of emission reductions.

Global chemical-transport models (GCTMs) have been widely used to study regional air pollution and resulting impacts from global climate and emission changes (Fiore et al., 2002; Mickley et al., 2004; Fiore et al., 2005; Murazaki and Hess, 2006; Lin et al., 2008a,b). They fully account for the long-range transport and stratosphere–troposphere exchange of pollutants, both of which have important consequences on regional air quality (Zhang et al., 2006a,b; Appel and Gilliland, 2007; Huang et al., 2008; Wuebbles et al., 2007; Lin et al., 2008b; Lefohn et al., 2001; Tarasick et al., 2007). Therefore GCTMs are able to integrate the contributions from global climate and emissions variations and changes to provide lateral boundary conditions that drive regional models to address regional air quality problems.

For regional studies, however, GCTMs are usually focused on pollutant concentrations during the daytime. They have not been examined for diurnal variations of pollutants due to concerns about the use of coarse spatial resolution, crude emissions specification, and/or oversimplified PBL mixing representation (Fiore et al., 2002; Mickley et al., 2004; Murazaki and Hess, 2006). Certainly, current GCTMs with a typical horizontal resolution of $2 \times 2.5^\circ$ or coarser cannot resolve a wide range of smaller scales where interactive atmospheric and surface processes play significant roles in pollutant spatial distributions and temporal variations. Meanwhile, the existing global emissions specified in GCTMs contain large errors from inadequate information on local emission activities and include only monthly mean distributions without diurnal and daily variations. More importantly, as discussed below, the PBL mixing representation in GCTMs is often oversimplified, causing substantial model biases in chemical species in the boundary layer and at the surface.

Continuous efforts have been made to improve the PBL mixing representation in air quality modeling. A brief summary of the PBL mixing schemes used in mesoscale chemistry models can be found at http://www.mi.uni-hamburg.de/Mesoscale-transport-or-chemistry-transport-model.676.0.html. They can be separated into two broad categories, based respectively on predictive turbulent kinetic energy (TKE, e.g., Mellor and Yamada, 1982) and diagnostic local or non-local *K*-theory (e.g., Holtslag and Boville, 1993) parameterizations. The PBL mixing is usually parameterized in terms of TKE or stability functions. Regional air quality models generally incorporate multiple PBL schemes of both categories, facilitating sensitivity studies of their impacts (e.g., Zhang et al., 2001; Ku et al., 2001). On the other hand, most current GCTMs adopt only a single local or non-local *K*-theory scheme, or even assume very simple mixing. For example, the GEOS-Chem (one of the most widely used GCTMs) assumes a fully mixed PBL throughout the day (Fiore et al., 2002; Fiore et al., 2005; Wu et al., 2007), thus likely overestimates vertical mixing in the case of stable or neutral conditions. The lack of multiple alternative schemes may explain why the sensitivity of GCTMs' simulations, especially of the pollutant diurnal cycle, to the PBL mixing representation is missing in the literature.

This study conducts a suite of GCTM sensitivity experiments to simulate the surface ozone diurnal cycle over the contiguous U.S. in summer 1999 and evaluate the impacts of PBL mixing representation, horizontal resolution, and emissions specification. The GCTM used here is the Model for Ozone And Related chemical Tracers version 2.4 (MOZART-2.4), with two important modifications in model chemistry/physics. Three major types of PBL mixing representations are compared, including a non-local scheme, a local scheme and a full-mixing assumption. Two resolutions are tested: T62 ($\sim 1.9^\circ$) and T106 ($\sim 1.1^\circ$), with the latter much higher than previous GCTM studies (Fiore et al., 2002; Mickley et al., 2004; Murazaki and Hess, 2006; Lin et al., 2008a,b; Wu et al., 2007). Our choice for the simulation in 1999 is partly because the ozone pollution in that summer was the worst since 1993 (the start of U.S. EPA data records available at http://www.epa.gov/ttn/airs/airsaqs/detaildata/downloadaqsdata.htm). Section 2 describes the model and experiment design. Section 3 presents our results on the diurnal variation of surface ozone and ozone vertical profiles in the lower troposphere. Section 4 further evaluates the model performance on daytime ozone. Section 5 concludes our findings.

2. Model and experiment design

2.1. Model

MOZART-2.4 (described and evaluated in detail by Horowitz et al. (2003)) is a state-of-the-art GCTM for studying tropospheric distributions and processes affecting ozone (e.g., Wuebbles et al., 2001; Wei et al., 2002; Horowitz et al., 2003; Lamarque et al., 2005; Murazaki and Hess, 2006; Lin et al., 2008a,b). Using meteorological data and chemical emissions as inputs, it simulates 63 species and 135 gaseous reactions, with 26 species undergoing heterogeneous processes (e.g., wet deposition), in the troposphere. MOZART integrates in order the advection, surface emission and deposition, vertical diffusion, convection, cloud and precipitation, and chemistry. Through a simple preprocessor manipulation, it can be run at various horizontal and vertical resolutions determined by the meteorological inputs.

2.2. The non-local PBL mixing scheme

To simulate the vertical mixing processes in the PBL, MOZART adopts by default the non-local mixing scheme formulated by Holtslag and Boville (1993):

$$\overline{w'C'} = -K_c(\partial C/\partial z - \gamma_c) \quad (1.1)$$

$$K_c = kw_t z(1 - z/h)^2 \quad (1.2)$$

$$\gamma_c = aw_* \overline{(w'C')}_0/(w_m^2 h) \quad (1.3)$$

$$h = \mathrm{Ri}_{cr}\left(u(h)^2+v(h)^2\right)\Big/((g/\theta_s)(\theta_v(h) - \theta_s)) \quad (1.4)$$

Where $\overline{w'C'}$ is the vertical mixing flux of a given atmospheric chemical tracer (with the mixing ratio of C) at model layer interfaces within the PBL, with the surface flux of $\overline{(w'C')}_0$, K_c is the eddy diffusivity, γ_c is the non-local term, and h is the PBL height. In the formulation of these terms, $\partial C/\partial z$ is the vertical gradient of the given tracer, k is the von Kármán constant, w_t and w_m are characteristic turbulent velocity scales with respect to tracers and momentum, respectively, z is the height of a model layer midpoint above the ground, a is a constant (i.e., 7.2), w_* is the convective velocity scale, Ri_{cr} is the critical Richard number, $u(h)$ and $v(h)$ are horizontal wind components at h, g/θ_s is the buoyancy parameter (g is the acceleration of gravity, and θ_s is an appropriate potential temperature of air near the surface), and $\theta_v(h)$ is the virtual potential temperature at h. More details can be found in Holtslag and Boville (1993). A similar non-local scheme by Hong and Pan (1996) is used as a major PBL scheme in the mesoscale weather model MM5. The Hong and Pan (1996) scheme is based on Holtslag and Boville (1993), with changes mainly on the calculation of w_t and w_m.

The non-local scheme accounts for the effects of not only the local gradients of chemical species but also their PBL-wide mixing by large-scale eddies when the PBL is convectively unstable. It requires the input of air temperature, water vapor, winds, surface heat and water vapor fluxes, and surface wind stresses to calculate various quantities determining the PBL mixing, including the PBL height, a non-local mixing term and eddy diffusivity. The detailed procedure to calculate these PBL mixing parameters can be found in Holtslag and Boville (1993). Here we briefly describe the procedure. First, h is calculated through iterating a formula equivalent to Eq. (1.4), $\mathrm{Ri} = h^*((g/\theta_s)(\theta_v(h)-\theta_s))/(u(h)^2 + v(h)^2)$, over the height from the surface to the upper troposphere, and is determined when the diagnosed bulk Richard number, Ri, is not less than Ri_{cr}. Then, K_c and γ_c are calculated through Eq. (1.2)–(3), based on h and other parameters. Finally, $\overline{w'C'}$ is calculated through Eq. (1.1). It is noted that γ_c takes effect only in the statically unstable PBL (i.e., the sum of surface sensible and latent heat fluxes into the atmosphere is positive), where it, together with K_c, distributes surface fluxes of chemical tracers, including emissions and dry depositions, into different model layers within the PBL, representing the PBL-wide transporting effects of large turbulent eddies.

Under the non-local scheme, the modeled PBL states vary widely from unstable in the afternoon to stable in the nighttime. Holtslag and Boville (1993) demonstrated that, different from local mixing schemes, the non-local scheme generated greater and more realistic vertical mixing of potential temperature, water vapor and cloud water. Their findings are also consistent with Zhang et al. (2001), who compared the local and non-local schemes using the mesoscale model MM5. On the other hand, the full-mixing assumption adopted by other major GCTMs such as GEOS-Chem is unable to simulate the stable and neutral conditions. As demonstrated in Section 3, the non-local scheme is critical for simulating the diurnal cycle of surface ozone.

2.3. Other PBL mixing schemes

To examine the impacts of PBL mixing representations on MOZART-2.4 simulations, two other PBL schemes are compared here with the default non-local scheme. The first scheme is a local mixing scheme used by Holtslag and Boville (1993) for comparing with their non-local scheme:

$$\overline{w'C'} = -K_c(\partial C/\partial z) \quad (2.1)$$

$$K_c = l_c^2 S F_c(R_i) \quad (2.2)$$

$$l_c = \left((kz)^{-1}+\lambda_c^{-1}\right)^{-1} \quad (2.3)$$

$$\lambda_c = 300 \text{ if } z < 1000\text{m} \;;$$
$$\lambda_c = 30 + 270e^{(1-z/1000)} \text{ if } z \geq 1000\text{m} \quad (2.4)$$

where l_c is a length scale, λ_c is a so-called asymptotic length scale, S is the local wind shear, and $F_c(R_i)$ is a stability function. (Other parameters are the same as those defined in the non-local scheme.) Under this scheme, λ_c, l_c, K_c and $\overline{w'C'}$ are calculated sequentially through the Equation set (2.1)–(2.4). Detailed descriptions of the local scheme can be found in Holtslag and Boville (1993).

The second scheme for comparing with the non-local scheme is the assumption of full-mixing PBL. It assumes that every chemical tracer is fully mixed (i.e., the mixing ratio, emission, and/or dry deposition have zero vertical gradient) below the PBL height, which is calculated the same way as is done under the non-local scheme.

2.4. Model modifications

In this study, two major modifications in model chemistry and physical parameterizations are incorporated into MOZART-2.4. They have been implemented in Lin et al. (2008a,b), but are described here in more detail. The first modification is for the isoprene chemistry. Previous sensitivity studies indicated that the modeled ozone formation was significantly affected by the representation of isoprene chemistry (von Kuhlmann et al., 2004; Fiore et al., 2005; Wu et al., 2007). The original MOZART-2.4 (i.e., that without the modifications incorporated here) assumes an 8% yield of isoprene nitrates through reactions between

nitric oxide and isoprene-derived peroxyl radicals, which then react with the hydroxyl radical (OH) to completely recycle nitrogen oxides ($NO_x = NO + NO_2$) rather than converting to nitric acid as a permanent sink of NO_x. Several observational/experimental analyses (Chen et al., 1998; Chuong and Stevens, 2002; Sprengnether et al., 2002) and model sensitivity evaluations (Fiore et al., 2005; Wu et al., 2007) have suggested that the yield of isoprene nitrates and the rate of conversion from isoprene nitrates to nitric acid may be underestimated in the original MOZART-2.4. In contrast, the observational analyses by Horowitz et al. (2007) suggested the best estimate of isoprene nitrate yield to be 4%, of which 40% was recycled back to NO_x, based on the comparison between the simulated and the observed alkyl nitrates within the PBL during an aircraft measurement campaign. The Horowitz et al. (2007) result, however, may have been compromised by the significant overestimation (up to about 70%) of isoprene concentrations in the PBL. Based on this, we feel it is more realistic to use a higher isoprene nitrate yield and conversion rate than used in the original MOZART-2.4. The present study adopts a 12% yield of isoprene nitrates, which is then converted completely to nitric acid, following Fiore et al. (2005) and Wu et al. (2007).

The second modification relates to ozone dry deposition. MOZART does not calculate dry deposition velocities interactively. Instead, it uses monthly mean dry deposition velocity data for ozone, nitrogen species and other chemicals calculated offline using the resistance-in-series scheme by Wesely (1989) (referred to as the Wesely scheme hereafter) driven by the National Centers for Environmental Prediction (NCEP)/National Center for Atmospheric Research (NCAR) reanalysis data. For ozone, a diurnal variation is imposed upon the prescribed monthly data during the model integration (Brasseur et al., 1998). Recent observational analyses (Padro, 1996; Zhang et al., 1996) and inter-model comparisons (Padro, 1996; Zhang et al., 1996; Wesely and Hicks, 2000 and references therein) suggest that the summertime dry deposition of ozone calculated by the Wesely scheme could be underestimated by about 30–80% over the deciduous forest prevailing in the eastern U.S. Therefore we increase the ozone dry deposition velocity by 30% in the summer months over the eastern U.S. (east of 100°W). This uniform increase is certainly very simplified since the actual underestimation with the Wesely scheme may have a large range as a result of the variability in vegetation types and meteorological conditions. Given that the ozone dry deposition velocity over forest is generally larger than those over other land types (Padro, 1996 and references therein; Zhang et al., 1996), the increase of 30% is reasonable and more likely conservative for most of the eastern U.S., with its significant forest coverage, although it may be overestimated at those locations with little forest coverage. Moreover, our analyses suggest that even in areas of possible overestimation, there is no significant impact on the modeled diurnal pattern of ozone variation.

The above two modifications substantially reduce the modeled surface daily 8-h maximum (D8hM) ozone concentrations over the eastern U.S. averaged over the 1999 summer. Fig. 1 shows that, as compared to the original model, the modified isoprene chemistry reduces the D8hM ozone by 8–14 ppb over the Southeast and 4–8 ppb over other regions of the eastern U.S. The 30% increase for ozone dry deposition velocity reduces the D8hM ozone by 4–6 ppb over the central eastern and northeastern U.S. and 2–4 ppb over other regions of the eastern U.S. Overall, incorporating the two modifications together, the modeled D8hM ozone are reduced by 6–18 ppb over the eastern U.S. and 2–6 ppb over the western U.S. Although the modified model still produces 5–44 ppb larger surface ozone concentrations than the surface measurements from the U.S. Environmental Protection Agency Air Quality System

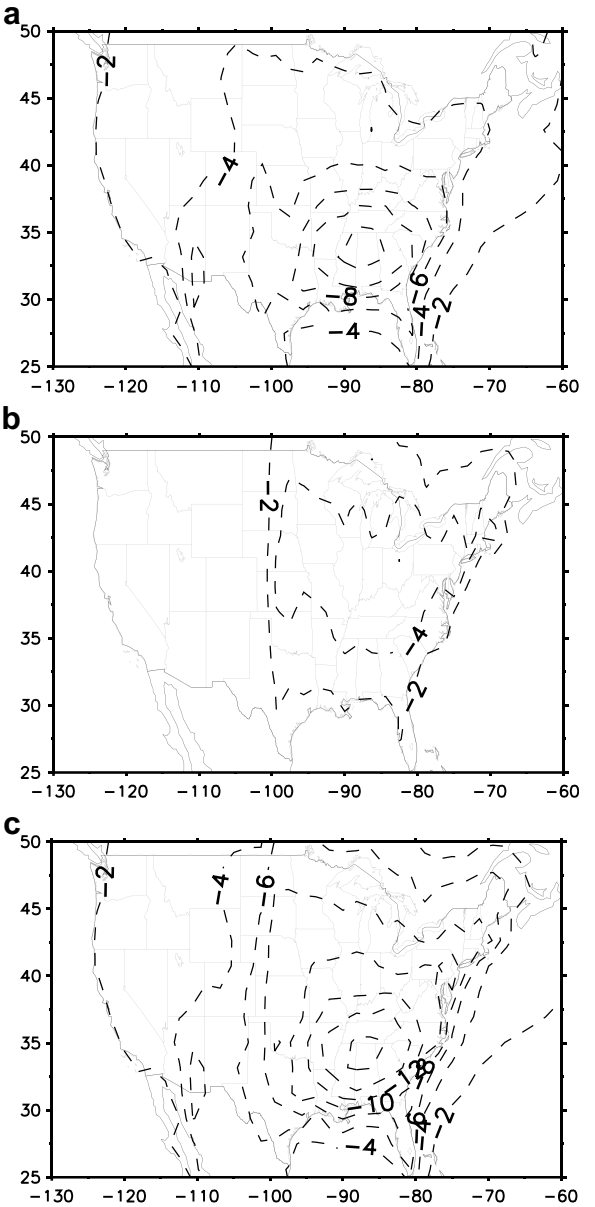

Fig. 1. Differences in the simulated surface D8hM ozone concentrations over the U.S. in summer 1999 between the original MOZART-2.4 and the model with modifications in (a) isoprene nitrate chemistry, (b) ozone dry deposition, and (c) both. The contour interval is 2 ppb.

(Fig. 5c, see Section 4 for more analyses) over the eastern U.S., the two model modifications did reduce the biases by 6–18 ppb over the same region.

Note that the two modifications incorporated here are subject to limitations in the current understanding of the corresponding aspects of atmospheric physics/chemistry. For example, there are still debates on the isoprene nitrate chemistry (Horowitz et al., 2007); and the dry deposition of ozone highly depends on the vegetation types and meteorological conditions. Further research, especially direct measurements, is required to enhance our understanding of these issues. Nevertheless, the two modifications improve the simulation of ozone distribution. Hereafter, we refer to the results from the modified MOZART unless otherwise stated.

2.5. Meteorological and emission inputs

MOZART is driven by meteorological data including air temperature, water vapor, winds, surface heat and water vapor fluxes, surface wind stresses, surface pressure, surface geopotential height, and land–sea-ice mask. This study uses two assimilated meteorological datasets at 6 h intervals, differing only in horizontal resolution of T62 ($\sim$1.9°) versus T106 ($\sim$1.1°), from the European Center for Medium range Weather Forecasting (ECMWF) ERA-40 (Uppala et al., 2005; available at http://dss.ucar.edu/catalogs/free.html). There are 60 vertical layers, with 13 layers below 800 hPa and the lowest layer centered at about 12 m above the ground. MOZART interpolates linearly the 6-h meteorological data to each time step during integration.

Two monthly datasets for surface emissions of ozone precursors are used in this study: (1) the Precursors of Ozone and their Effects in the Troposphere (POET, Granier et al., 2005), and (2) the 'MOZ2' dataset from the previous MOZART-2.4 (see details in Horowitz et al., 2003). The two datasets are often used in the simulations of MOZART (e.g., Wuebbles et al., 2001; Horowitz et al., 2003; Tie et al., 2005; Lin et al., 2008a,b).

Both POET and MOZ2 contain emissions of ozone precursors, including NO_x, carbon monoxide (CO) and volatile organic compounds (VOC) from anthropogenic (fossil fuel, transportation, industrial, and biofuel) and natural (biomass burning, biogenic/soil and oceanic) sources. Anthropogenic emissions in POET and MOZ2 are based on the Emission Database for Global Atmospheric Research version 3 (EDGAR-3) and version 2 (EDGAR-2), respectively. They have been used by more than 700 users worldwide since their establishments (Olivier et al., 2001). Relative to EDGAR-2, EDGAR-3 contains improved representation of anthropogenic emission sources, including the improved emissions from agricultural waste burning, the updated emission factors for industry and transportation, and the updated maps of population and industrial sectors (Olivier et al., 2001; also available at http://www.mnp.nl/edgar/documentation/differences/).

For biomass-burning emissions, the amount of biomass burned is estimated based on the climatology by Hao and Liu (1994), and the emission factors are based on Andreae and Merlet (2001). In MOZ2, the burned biomass in the extratropics is based on Müller (1992). Following Lin et al. (2008a,b), biofuel and biomass burning emissions of CO in both datasets are scaled up around 1.5 times to generate a global budget (about 1550 Tg yr^{-1} from all sources) comparable to the estimate in the Intergovernmental Panel on Climate Change (IPCC) Third Assessment Report (TAR) (IPCC, 2001). The impact of this scaling upon the surface ozone simulation, however, is less than 1 ppb, often less than 0.5 ppb, over the U.S. (not shown). Biogenic emissions in POET are adopted from the Global Emissions Inventory Activity (GEIA) (e.g., Guenther et al., 1995) for VOC and Müller and Brasseur (1995) for CO. Biogenic emissions in MOZ2 are from multi sources including GEIA (see details in Horowitz et al., 2003). Soil emissions of NO_x are taken from Yienger and Levy (1995) in both POET and MOZ2.

Over the U.S., summer anthropogenic emission budgets for NO_x and CO in POET are about 1.46 Tg N and 23.6 Tg, respectively, which are comparable with the budgets from the U.S. 1999 National Emission Inventory (NEI99) ($\sim$1.58 Tg N, and 26.1 Tg, respectively; assuming one fourth

Table 1
Experiment design

Experiment	Emissions	Meteorology	PBL mixing scheme
M_control	POET	ERA-40/T62	Non-local scheme
M_LS	POET	ERA-40/T62	Local scheme
M_LS_30 m	POET	ERA-40/T62	Local scheme, with the asymptotic length scale set as 30 m
M_FM	POET	ERA-40/T62	Fully mixing
M_FM_1 km	POET	ERA-40/T62	Fully mixing, with the minimum PBL height set as 1000 m
M_T106	POET	ERA-40/T106	Non-local scheme
M_MOZ2	MOZ2	ERA-40/T62	Non-local scheme
M_no2xoh[a]	POET	ERA-40/T62	Non-local scheme

[a] The rate constant of the reaction $NO_2 + OH + M \rightarrow HNO_3 + M$ is increased by 50%.

Table 2
Evaluation of the simulated D8hM ozone in summer 1999 over the western and eastern U.S. (separated by 100°W)[a]

Experiment	# of Sites	Obs. (ppb)	Mod. (ppb)	MB (ppb)	MAGE (ppb)	RMSE (ppb)	NMB	NME	MNGE
Western U.S.									
M_control	130	52.3	52.3	1.0	9.2	12.1	2%	18%	20%
M_LS	130	59.7	59.7	8.4	13.2	18.7	16%	26%	28%
M_LS_30 m	130	61.7	61.7	10.3	14.5	20.3	20%	28%	31%
M_FM	130	53.0	53.0	1.7	9.0	12.1	3%	18%	20%
M_FM_1 km	130	53.4	53.4	2.0	8.7	11.4	4%	17%	19%
M_T106	130	52.2	52.2	0.9	9.2	11.7	2%	18%	21%
M_MOZ2	130	50.7	50.7	−0.6	8.9	11.0	−1%	17%	19%
M_no2xoh	130	46.9	46.9	−4.5	10.1	12.4	−9%	20%	20%
Eastern U.S.									
M_control	321	56.2	69.3	13.1	13.3	15.5	23%	24%	25%
M_LS	321	56.2	71.4	15.1	15.8	20.1	27%	28%	30%
M_LS_30 m	321	56.2	74.2	18.0	18.5	23.0	32%	33%	35%
M_FM	321	56.2	70.7	14.4	14.5	16.4	26%	26%	27%
M_FM_1 km	321	56.2	72.0	15.7	15.8	17.5	28%	28%	29%
M_T106	321	56.2	68.4	12.1	12.3	13.7	22%	22%	23%
M_MOZ2	321	56.2	70.8	14.6	14.7	16.7	26%	26%	28%
M_no2xoh	321	56.2	63.3	7.1	8.1	10.4	13%	14%	16%

[a] See Section 2.5 for definitions of the evaluation metrics.

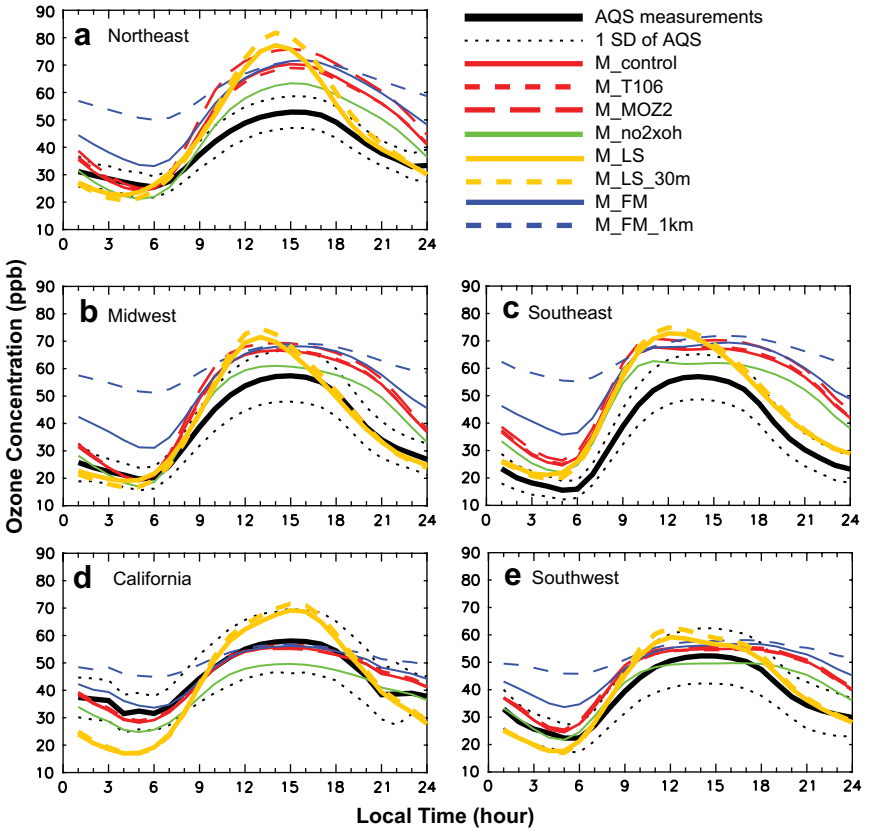

Fig. 2. Summer average diurnal cycle of surface ozone concentrations in 1999 over the five U.S. regions. The dotted lines denote one standard deviation of the EPA AQS rural site measurements during 1996–2000. See Fig. 5a for regional specifications.

of the annual budgets are emitted in summer; available at http://www.epa.gov/ttn/chief/trends/). The U.S. emission budgets in MOZ2 differ from POET by less than 8% for anthropogenic sources and 6% for all sources. However, the geographical distributions of precursor emissions over the U.S. are very different between POET and MOZ2, with the emissions much more concentrated in major source locations (large cities, power plants, etc.) in the former than the latter dataset (not shown).

Table 3
The differences between the daily maximum and minimum surface ozone concentrations in summer 1999 over the five U.S. regions

Experiment	Northeast	Midwest	Southeast	California	Southwest
Observation	27.3	37.7	41.4	26.5	30.0
M_control	18.9[a]	9.9	1.6	0.9	0.4
M_LS	27.3	14.8	10.2	25.7	11.5
M_LS_30 m	33.8	20.3	13.7	28.0	15.5
M_FM	11.2	−0.6	−7.9	−4.0	−6.9
M_FM_1 km	−5.6	−19.8	−24.8	−14.7	−17.7
M_T106	16.8	10.4	1.3	1.1	0
M_MOZ2	23.4	12.7	3.0	0.3	0.2
M_no2xoh	14.9	6.4	−0.8	−1.6	−2.0

[a] The values corresponding to each model experiment are their biases from the EPA AQS rural site measurements, i.e., the modeled difference between daily ozone maximum and minimum minus the observed difference. Positive values denote that the model over predicts the difference between daily ozone maximum and minimum.

2.6. Experiment design

Table 1 specifies the eight experiments used in this study. In particular, the control experiment, M_control, is driven by the ERA-40/T62 data with the POET emissions and the non-local PBL mixing scheme. To evaluate the impacts of PBL mixing schemes on the simulation of ozone diurnal cycle, we compare M_control with the sensitivity experiments using the local mixing scheme (M_LS and M_LS_30 m) and the full-mixing assumption (M_FM and M_FM_1 km). The experiment M_LS adopts the local scheme, while M_LS_30 m slightly adjusts the local scheme by setting a constant of 30 m for the asymptotic length scale λ_c throughout the troposphere. This value is appropriate for the free troposphere yet too small for the PBL (Holtslag and Boville, 1993), resulting in weaker PBL mixing in M_LS_30 m than M_LS. The experiment M_FM assumes a full-mixing PBL. The experiment M_FM_1 km is similar to M_FM, except that the minimum PBL height is arbitrarily set as 1000 m, resulting in much stronger PBL mixing during the nighttime. As shown in Section 3, the experiments M_LS_30 m and M_FM_1 km serve as some extreme cases for the local mixing scheme and the full-mixing assumption, respectively.

In addition, the experiments M_T106 and M_MOZ2 are used to evaluate the model sensitivity to horizontal resolution and emissions specification, respectively. They are

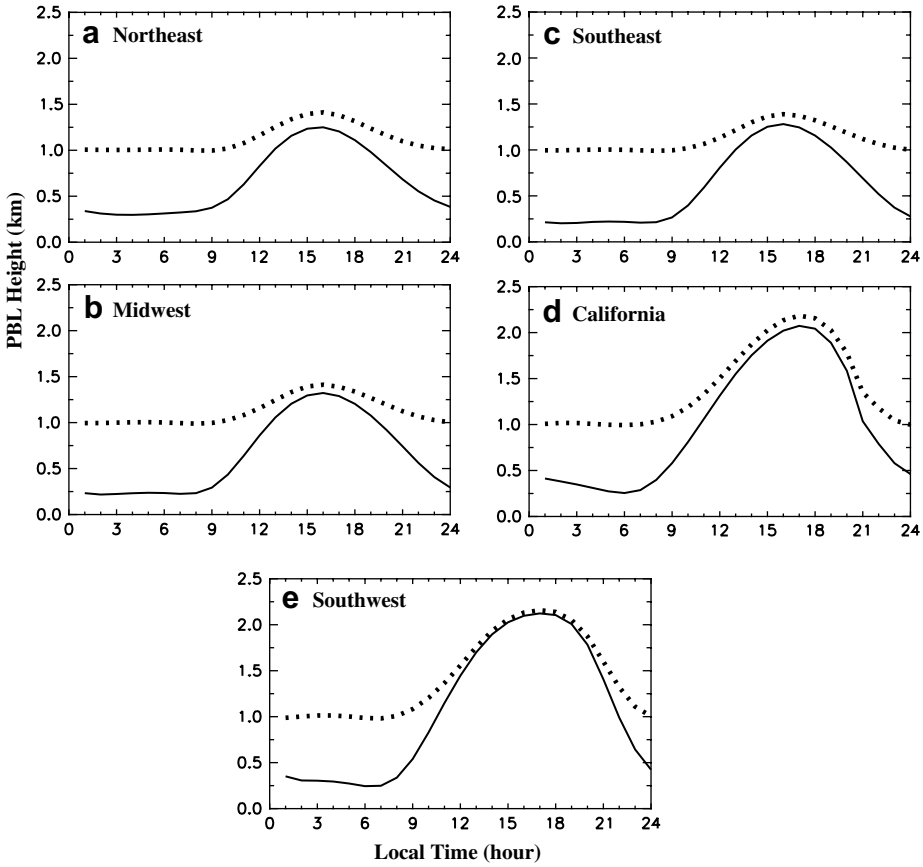

Fig. 3. Summer average diurnal variation of planetary boundary layer heights in 1999 calculated by MOZART over the five U.S. regions. The solid lines are for M_control and the dashed lines are for M_FM_1 km. See Fig. 5a for regional specifications.

similar to M_control, except that the ERA-40/T106 meteorological data and the MOZ2 emissions data are used, respectively.

Finally, the experiment M_no2xoh is conducted to evaluate the impact of ozone production efficiency. It is similar to M_control, except for an increase of 50% to the rate constant of $NO_2 + OH + M \rightarrow HNO_3 + M$, one major termination mechanism for the chain reactions of daytime photochemistry associated with ozone formation. Through this manipulation, the ozone production efficiency can be reduced by as large as 33% assuming the chain reactions are terminated only by this specified mechanism. This has significant consequences on the simulation.

Note that the ozone phenomena at urban or smaller scales cannot be resolved in the present experiments, even when using the ERA-40/T106 data. Nonetheless, our model resolutions are much higher than those in recent global modeling studies of ozone and/or other pollutants over the U.S. (Fiore et al., 2002; Mickley et al., 2004; Fiore et al., 2005; Murazaki and Hess, 2006; Lin et al., 2008a,b).

2.7. Statistical metrics for model sensitivity evaluation

Several statistical metrics are used here to evaluate the model sensitivity for the D8hM ozone to various PBL mixing schemes, spatial resolutions and precursor emissions datasets for both the western and eastern U.S. (Table 2). The two regions are separated by an artificial boundary at 100°W. The evaluation metrics are applied to the Environmental Protection Agency (EPA) Air Quality System (AQS) rural measurement sites. Urban measurement sites are not included as the relatively coarse global model precludes the resolution at urban or smaller scales. Following the guidance of U.S. EPA (1999,2001) and Seigneur et al. (2000), the evaluation metrics examined here (see Eq. set (3)) include mean bias (MB), mean absolute gross error (MAGE), root mean square error (RMSE), normalized mean bias (NMB), normalized mean gross error (NME), and mean normalized gross error (MNGE). In particular, the MB and NMB represent the systematic error for the modeled ozone over the specified measurement sites and its relative scale to the observed measurement site-wide mean, respectively. The MAGE and NME represent the mean unsigned error for the modeled ozone over the specified measurement sites and its relative scale to the observed measurement site-wide mean, respectively. The RMSE is similar to the MAGE, but it emphasizes the importance of the measurement sites with larger unsigned errors more than the importance of the measurement sites with smaller unsigned errors. The MNGE is similar to NME, but it represents the mean of

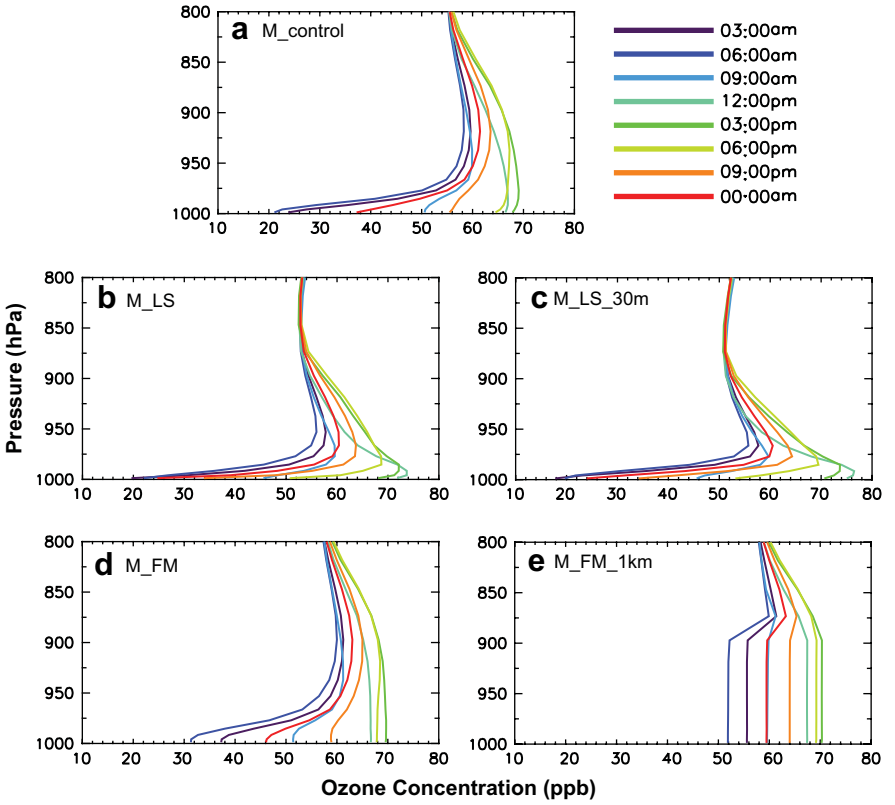

Fig. 4. Summer average ozone vertical profiles at different times of day below 800 hPa in 1999 over the Midwest. See Fig. 5a for regional specifications.

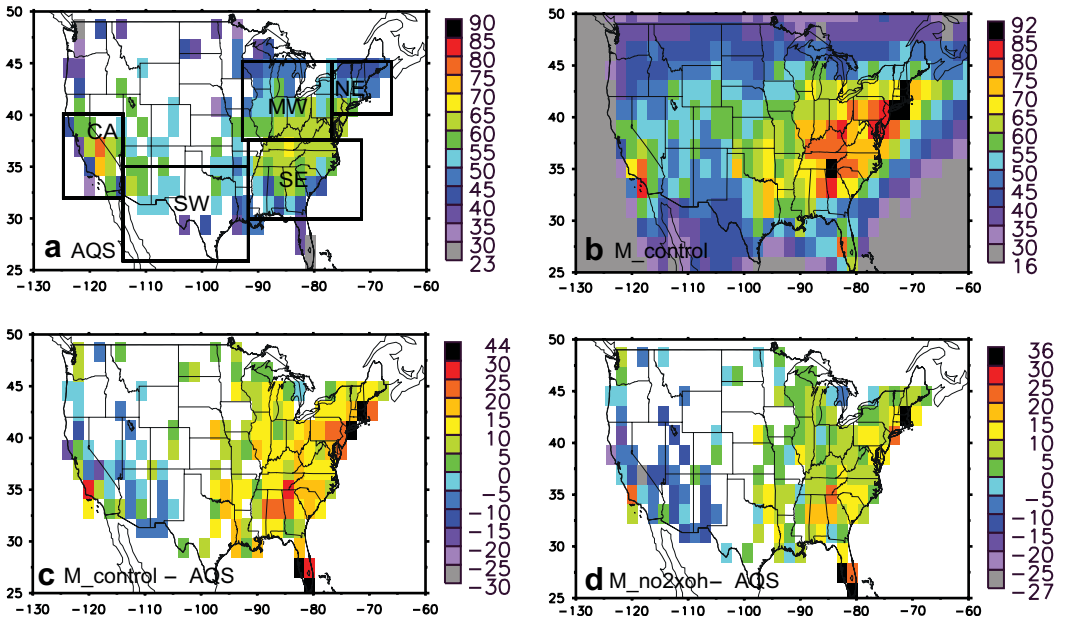

Fig. 5. Summer average daily 8-h maximum concentrations of surface ozone in 1999 over the U.S. from (a) the EPA AQS rural site measurements and (b) M_control; and (c,d) differences between model experiments and measurements. The units are ppb. Positive values in (c,d) depict overestimations in the model experiments. Superimposed in (a) is the specification of the five regions for calculating diurnal variations of ozone and PBL height in Figs. 2–4: Northeast (NE), Midwest (MW), Southeast (SE), California (CA), and Southwest (SW); in each region, only the model grid boxes with available ozone measurements are taken into account in the calculation.

the normalized unsigned errors over the specified measurement sites. These evaluation metrics are widely used in previous studies (e.g., Zhang et al., 2006a; Huang et al., 2007).

$$\begin{aligned} M_{\text{obs}} &= \tfrac{1}{N}\textstyle\sum_{i=1}^{N} C_{\text{obs},i} \\ \text{MB} &= \tfrac{1}{N}\textstyle\sum_{i=1}^{N}\left(C_{\text{mod},i} - C_{\text{obs},i}\right) \\ \text{MAGE} &= \tfrac{1}{N}\textstyle\sum_{i=1}^{N}\left|C_{\text{mod},i} - C_{\text{obs},i}\right| \\ \text{RMSE} &= \sqrt{\tfrac{1}{N}\textstyle\sum_{i=1}^{N}\left(C_{\text{mod},i} - C_{\text{obs},i}\right)^2} \\ \text{NMB} &= \text{MB}/M_{\text{obs}} \\ \text{NME} &= \text{MAGE}/M_{\text{obs}} \\ \text{MNGE} &= \tfrac{1}{N}\textstyle\sum_{i=1}^{N}\left|\left(C_{\text{mod},i} - C_{\text{obs},i}\right)\right)/C_{\text{obs},i}\right| \end{aligned} \tag{3}$$

where N is the number of measurement sites; $C_{\text{obs},i}$ and $C_{\text{mod},i}$ are the observed and the modeled ozone concentrations at each site, respectively.

3. Ozone diurnal cycle

The analysis below focuses on the regional mean diurnal variation of ozone over five major U.S. regions: Northeast, Midwest, Southeast, California and Southwest (see boundary specifications in Fig. 5a). These regions have often been identified with significant concerns on high ozone levels. They were also investigated by Lin et al. (2008a) for future ozone projections over the coming century in response to changes in climate and biogenic precursor emissions.

Fig. 2 presents summer 1999 mean surface ozone diurnal cycle averaged over the five regions derived from the EPA AQS rural site measurements and model simulations. Over the five regions, the observed ozone maximizes around 3:00 pm and minimizes around 6:00 am. The ozone maxima are 26–42 ppb, or 1.5–4 times, larger than the minima (Table 3).

The observed timing of the ozone maximum and minimum is realistically simulated in M_control, with the phase shift less than 1 h (Fig. 2). The model biases for the ozone maximum are about 10–20 ppb over the eastern U.S. and less than 5 ppb over the western U.S. (see also Table 2 for the D8hM ozone). For the ozone minimum, the biases are less than 5 ppb, except over the Southeast. Overall, the contrast between ozone maximum and minimum is overpredicted by 18.9 ppb for the Northeast and by 9.9 ppb for the Midwest, but is within 2 ppb of the observed for the Southeast, California and the Southwest (Table 3).

Since daily ozone variation is affected by the variation of PBL height, we examine the PBL height simulated by the non-local scheme (Fig. 3, solid black lines). The daily maximum PBL height occurring in the afternoon is about 1–1.5 km in the Northeast, Midwest and Southeast, and 2–2.2 km in California and the Southwest, which is consistent with the study of Fiore et al. (2002), see their Fig. 1b) for 1995 July. Previous studies suggest that the non-local scheme may overestimate the PBL height (e.g., Zhang et al., 2001). To test the impacts of possible inaccuracies in the modeled PBL height on the simulated ozone variation, two sensitivity experiments (in additional to those described in Section 2.6 and Table 1) are done here, where the PBL height is artificially increased and decreased 30%, respectively, at any given time. For a given region, the resulting impacts on ozone concentrations maximize during the peak ozone period and negligible (i.e., < 1 ppb) in the nighttime (not shown). The largest impact among the five regions is on the ozone maximum over the Northeast, where increasing (decreasing) the PBL height reduces (enhances) the ozone concentrations by about 3–5 ppb. Note that the two sensitivity experiments only test the likely inaccuracies in the PBL height formulation, and do not take into account the concurrent inaccuracies in the formulation of other parameters (including the eddy diffusivity).

Over the diurnal cycle, the largest ozone bias in M_control is found at the time of ozone decline in the early evening. Specifically, ozone destruction occurs rapidly during 6:00 pm–9:00 pm in observations but much slower in M_control. This may be because the simulated PBL mixing is too strong, causing stronger downward transport of ozone from the upper PBL and weaker NO_x titration as NO_x is transported upward. Fig. 3 shows that the simulated PBL top is as high as 0.7–1.2 km during 6:00 pm–9:00 pm over the Northeast, Midwest and Southeast, 1–2 km over California, and 1.5–2.1 km over the Southwest. Although no observational data exist for verification, we speculate that the decline rate of the simulated PBL height in the early evening is likely underestimated, which may in part be due to the artificial linear interpolation of meteorological conditions from the only available 6-hourly ERA-40 data.

To further evaluate the role of PBL mixing in surface ozone variation throughout the day, we examine the diurnal variation of ozone vertical profile below 800 hPa over the Midwest in M_control (Fig. 4a). From midnight to early morning, ozone concentrations are reduced at all altitudes. Due to the stable and shallow PBL, however, the rate of ozone reduction decreases with height significantly. Near the surface, ozone is reduced greatly from 37 ppb at midnight to 24 ppb by 3:00 am and to 21 ppb by 6:00 am. At 950 hPa, by comparison, the ozone reduction is only about 4 ppb during the same time period. In the morning, the surface ozone concentration is increased rapidly by two causes. First, as solar radiation increases, the photochemistry takes place and ozone is formed quickly. Second, due to the surface heating, the PBL deepens (Fig. 3), the vertical mixing increases, and ozone at higher altitudes is transported down to the surface (see also Zhang and Rao, 1999). As a result, the surface ozone concentration is significantly increased from 21 ppb to 50 ppb by 9:00 am and to 66 ppb by noon. Meanwhile the ozone concentration at 950 hPa is only increased by 9 ppb as a result of the canceling between the downward transport and the in situ ozone formation. In the afternoon, ozone concentrations maximize at 63–69 ppb throughout the lower troposphere below 900 hPa with minor vertical gradient due to the strong mixing. During the early evening (6:00 pm–9:00 pm), ozone concentrations in the PBL are destroyed gradually, with the destruction only about 8 ppb near the surface and 5 ppb at 950 hPa. From 9:00 pm to midnight, however, the PBL is stabilized and the mixing weakened rapidly. The ozone concentration near the surface is reduced by as much as 19 ppb during the 3-h period due to NO_x titration and dry deposition. By comparison, the reduction at 950 hPa is only

3 ppb due to the lack of a destruction mechanism, i.e., weak downward transport, small NO_x titration, and no dry deposition. Overall, the magnitude of ozone diurnal variation is as large as 47 ppb near the surface but only about 11 ppb at 950 hPa, 8 ppb at 900 hPa, and 2 ppb at 800 hPa. These comparisons indicate the central role of the PBL mixing on the ozone diurnal cycle and its vertical variation.

3.1. Sensitivity of the modeled ozone diurnal cycle to PBL mixing schemes

3.1.1. Effects of the local mixing scheme

M_LS and M_LS_30 m produce a much stronger diurnal cycle of surface ozone than M_control and observations due to the weaker PBL mixing during both daytime and nighttime (Fig. 2). In the afternoon with convectively unstable PBL, the ozone produced near the surface is not transported upward as efficiently as M_control; while during the nighttime, the downward ozone transport from the upper PBL is also weaker. Therefore, as compared to M_control, both experiments simulate a higher maximum (see also Table 2 for the D8hM ozone) and lower minimum, and thus a stronger diurnal cycle of ozone. The contrast between ozone maximum and minimum is overestimated by 10–28 ppb in M_LS and by 13–34 ppb in M_LS_30 m for the five regions (Table 3). Moreover, except for California, the timing of ozone maximum and minimum simulated in both experiments is 1–2 h earlier than those in M_control and observations. On the other hand, the ozone decline during the early evening in M_LS and M_LS_30 m is much more rapid than that in M_control (Fig. 2). This rapid decline is closer to observations, suggesting that the PBL mixing during the early evening may be too strong in M_control with the non-local scheme.

The local mixing scheme in M_LS also has significant consequences on the vertical distribution of ozone diurnal variation below 800 hPa (Fig. 4b,c). Over the Midwest, the ozone diurnal variation is strong only in a thin layer very close to the ground, i.e., below 975 hPa. Near the surface, the ozone concentration varies by as large as 52 ppb in a day, which is 5 ppb larger than M_control. The variation, however, is only about 10 ppb at 950 hPa and 5 ppb at 900 hPa, respectively about 1 ppb and 3 ppb smaller than M_control. Above 875 hPa, the diurnal variation of ozone is less than 2 ppb. In the afternoon, ozone concentrations decrease significantly with height at a rate of about 0.15 ppb hPa^{-1} between 990 hPa and 850 hPa. By comparison, the vertical variation of ozone concentrations in M_control is less than 3 ppb below 900 hPa at any time in the afternoon. In M_LS_30 m, the PBL mixing is weaker than M_LS, thus the ozone diurnal variation is larger near the surface and smaller at higher altitudes. Our results are consistent with Holtslag and Boville (1993) and Zhang et al. (2001), who found that the modeled vertical mixing was generally stronger and more realistic when the PBL-wide mixing by large-scale eddies was introduced, as in the non-local schemes.

The much weaker PBL mixing in M_LS and M_LS_30 m than M_control is caused by two factors. First, the local mixing scheme tends to produce a much shallower PBL and thus weaker interaction between the surface and higher altitudes. Holtslag and Boville (1993) found that the non-local scheme transported surface water vapor up to an altitude much higher than the local scheme, which trapped water vapor mostly in the layer close to the ground. Second, the meteorological variables from ERA-40 are generated using a non-local PBL scheme (Troen and Mahrt, 1986) similar to the one in M_control. When used to drive the local mixing scheme, they tend to cause the local scheme to generate much smaller eddy diffusivity (K_c) than the non-local scheme. This effect was analyzed in detail by Holtslag and Boville (1993), who found that the K_c derived from the local scheme was almost two orders of magnitude smaller than that from the non-local scheme when the meteorological variables based on the non-local scheme were used to drive the local scheme. The second cause also explains the relatively small difference in surface ozone diurnal cycle between M_LS and M_LS_30 m (Fig. 2): since the K_c is already rather small and pollutants are trapped in a very shallow PBL in M_LS, further reducing K_c has only a small impact on the vertical mixing.

3.1.2. Effects of the fully mixed PBL assumption

M_FM and M_FM_1 km produce a much weaker diurnal cycle of surface ozone than M_control due to the assumption of a fully mixed PBL (Fig. 2). In the nighttime, the ozone decline in M_FM and M_FM_1 km is much slower than M_control and observations because of weaker ozone destruction near the surface as well as more efficient addition of ozone from higher altitudes. First, NO_x emissions and ozone dry deposition are evenly distributed throughout the PBL, resulting in less ozone destruction through NO_x titration and dry deposition, respectively, near the surface. Second, given the increasing ozone concentration with height in the lower troposphere during the nighttime, the fully mixed ozone concentration throughout the PBL means that the higher ozone concentrations in the upper PBL are brought down to the surface much more efficiently than the case of stable PBL under the non-local scheme. In M_FM_1 km, these two effects are even more significant as the minimum PBL height is increased to 1000 m. In the afternoon, however, the simulated surface ozone concentrations in both M_FM and M_FM_1 km are similar to that in M_control (see also Table 2 for the D8hM ozone), despite the much larger ozone concentration in the early morning, from when the daytime ozone is accumulated. This is because the daytime ozone production near the surface in M_FM and M_FM_1 km is less than in M_control as precursor emissions are distributed throughout the PBL rather than concentrating near the surface. Overall, the contrast between ozone maximum and minimum is underpredicted by 0–8 ppb in M_FM, except over the Northeast; while the underestimation is about 5–25 ppb in M_FM_1 km over the five regions (Table 3).

Fig. 4d illustrates the diurnal variation of ozone vertical profiles over the Midwest in M_FM. Above 975 hPa, the vertical profiles of ozone are similar to M_control during most of the day. Below 975 hPa, however, ozone concentrations vary much less than M_control. The diurnal variation of surface ozone is only 37 ppb, about 78% of that in M_control. In the afternoon (12:00 pm–6:00 pm), the ozone profiles are similar to M_control, but with ozone

concentrations constant below 900 hPa at any time. For M_FM_1 km, there is no vertical gradient of ozone concentrations below 900 hPa at any time of the day and the daily variation of ozone is only about 18 ppb (Fig. 4e).

Note that, in M_FM during the nighttime, the seasonal and regional average PBL height are greater than 400 m over the Midwest (Fig. 3b, approximately equivalent to a PBL depth of 40 hPa (i.e., from 1000 hPa to 960 hPa)), thus one might expect little vertical gradient of simulated ozone concentrations below 960 hPa due to the full-mixing PBL assumption. However, the simulated vertical gradient of ozone is still very strong (Fig. 4d), which is primarily because of the interaction between the vertical gradient of ozone and the PBL height. Under the full mixing PBL assumption, surface ozone concentrations in the nighttime are very sensitive to the PBL height. A lower PBL height leads to a lower surface ozone concentration (due to more destruction and less transport from higher altitudes). By comparison, ozone concentrations at 960 hPa are not sensitive to the PBL height/mixing (in fact they are not sensitive to PBL mixing schemes (Fig. 4a,b,d)). In addition, the nighttime PBL height varies greatly from one location to another and from one day to another. For example, for any model grid box, the standard deviation of daily minimum PBL height during summer days is similar to its summer average. Therefore, in the case of shallow nighttime PBL, there is a large vertical gradient of ozone in the lower troposphere, while the full-mixing assumption is only applied to a thin layer much below 960 hPa; thus the surface ozone concentration is still much smaller than that at 960 hPa. In the case of deep nighttime PBL, on the other hand, the vertical gradient of ozone is much smaller in the PBL, thus the assumption of fully mixed PBL does not significantly affect the gradient below 960 hPa. As a result, assuming a fully mixed PBL during the nighttime, the ozone concentration at 960 hPa is affected insignificantly, while the surface ozone concentration is increased but is still smaller than that at 960 hPa; thus the vertical gradient of ozone below 960 hPa is reduced but not completely. As shown in Fig. 4, the difference in ozone concentrations near the surface and at 960 hPa is only 24 ppb at 6:00 am in M_FM as compared to 35 ppb in M_control. In M_FM_1 km, by comparison, the vertical gradient of ozone below 900 hPa disappears throughout the day since the PBL height is always 1000 m (approximately equivalent to a PBL depth of 100 hPa (i.e., from 1000 hPa to 900 hPa)) or larger at every location and time.

3.2. Sensitivity of the modeled ozone diurnal cycle to spatial resolution and emissions

M_T106 produces surface ozone diurnal variations similar to M_control when averaged over the five regions (Fig. 2, Table 3). The effect of increasing horizontal resolution from T62 to T106 on the production and destruction of ozone is significant for individual locations, but is largely canceled when averaging over a large area.

The diurnal pattern of surface ozone in M_MOZ2 is generally similar to M_control, while the bias is 1–6 ppb larger during most of the day over the eastern U.S. (Fig. 2). In addition, the contrast between daily ozone maximum and minimum is increased to 23.4 ppb over the Northeast and to 12.7 ppb over the Midwest (Table 3).

Over California, all the three experiments, M_control, M_T106, and M_MOZ2, successfully reproduce the observed diurnal variation of surface ozone (Fig. 2). The biases are less than 5 ppb throughout most of the day, except during the evening. The ozone minimum in the early morning is captured. Overall, it appears that the observed regional mean ozone diurnal cycle over California is well simulated regardless of the horizontal resolutions or emission inputs being used here.

4. Daytime ozone

For the diurnal cycle of ozone, its daytime level as a result of strong production through photochemistry is of most concern due to its great adverse impacts on human health, agriculture, and environment. On the other hand, large biases are persistent during the daytime over the three regions in the eastern U.S. (Fig. 2a–c). This section elaborates on the possible causes for the daytime biases.

Fig. 5a–c compare the modeled summer 1999 average surface D8hM ozone concentrations from M_control with the EPA AQS rural site measurements. If multiple rural measurement sites exist within a given model grid box, the observation data from them are averaged to facilitate the comparison with the modeled values, following Fiore et al. (2002); Murazaki and Hess (2006) and Lin et al. (2008a). The model captures the spatial pattern of ozone in general, with the highest level over the central and northeastern U.S. and southern California. Over most of the western U.S., the modeled ozone concentrations are comparable to the observed with biases less than 10 ppb. Over most of the eastern U.S., however, the ozone concentrations are over-predicted by 5–25 ppb. The largest biases, maximizing at 44 ppb, occur at several grid boxes associated with major cities located at the coasts of Florida and the Northeast since the model is not able to simulate the land–sea contrast of pollutant emissions and concentrations very well at the T62 resolution. Similar large biases are also seen in other coarse global models (e.g., Fiore et al., 2002). Increasing the horizontal resolution from T62 to T106 reduces the maximum bias to 32 ppb and has slighter impacts where model biases are smaller (not shown). The improvements with higher resolution here are consistent with Wild and Prather (2006), who found improved ozone simulations when the spatial resolution was increased from T21 (~550 km) to T42 (~300 km), T62 and T106.

Table 2 presents model ozone bias statistics for the western and eastern U.S. Over the western U.S., the five experiments M_control, M_FM, M_FM_1 km, M_T106 and M_MOZ2 are comparable, with the MB of −0.6 to +2.0 ppb, the MAGE of 8.7–9.2 ppb, and the RMSE of 11.0–12.1 ppb. M_LS and M_LS_30 m, however, produce much larger biases, i.e., 8.4–20.3 ppb. Over the eastern U.S., the MB, MAGE, and RMSE of ozone are 13.1–15.5 ppb in M_control. Relative to the biases in M_control, increasing the horizontal resolution from T62 to T106 slightly improves the simulation, reducing the MB by 1.0 ppb and the RMSE by 1.8 ppb. On the other hand, using the less accurate MOZ2 emission dataset leads to 1.2–1.4 ppb increases in the MB, MAGE and

RMSE for ozone. Incorporating the local PBL mixing scheme (M_LS and M_LS_30 m) increases the MB, MAGE and RMSE by 2.0–7.5 ppb, and the full-mixing assumption (M_FM and M_FM_1 km) increases the biases by 0.9–2.6 ppb. Overall, the model biases are much larger over the eastern than western U.S.

The large model biases for the daytime ozone persistent over the eastern U.S. are also found in previous MOZART simulations (e.g., Murazaki and Hess, 2006; Lin et al., 2008a). As discussed in Section 2.2, two aspects of the model chemistry/physics have been modified to improve the model performance on the daytime ozone. While other inaccuracies in model chemistry/physics and errors in emission/meteorological inputs may exist, another important cause is the model spatial resolution and its interactions with the significant precursor emissions over the eastern U.S. Even at T106, the size of a grid box over the U.S. is still about 10^4 km^2. Over the eastern U.S., ozone in the lower troposphere is primarily produced by the photochemistry involved with NO_x and VOC, whose relative abundances determine the efficiency of ozone production (Sillman, 1999). NO_x and VOC are mainly derived from surface emissions with significantly different temporal and spatial distributions, as the contributions of individual emission sources (e.g., power plants, industry, transportation, domestic, soil, biosphere) for NO_x differ from those for VOC. Due to the short atmospheric lifetimes, these precursors are often concentrated around their own emission source regions rather than distributing homogeneously across large areas. Therefore, in reality, there often exists 'mismatch' of NO_x and VOC concentrations within the region specified by a given model grid box, i.e., high NO_x concentrations with relatively low VOC concentrations at some locations, and vice versa in some other locations. This 'mismatch' occurs most significantly between NO_x and biogenic VOC but also between NO_x and anthropogenic VOC (e.g., ozone production is typically limited by VOC in large cities due to less VOC relative to NO_x, although there are significant amount of VOC). As a result, the efficiency of ozone production for that region is often not optimized due to the 'mismatch' between the concentrations of NO_x and VOC. In the simulations, however, the coarse spatial resolution, together with the usual assumption of subgrid homogeneity, results in instant mixing and therefore a closer 'match' of NO_x and VOC geographically, which artificially enhances the ozone production efficiency. Wild and Prather (2006) also found enhanced ozone production when the spatial resolution was decreased. Such effect is less significant over most of the western U.S. because of the relatively lower emissions of NO_x and/or VOC.

The impacts of model spatial resolution on MOZART simulations have been demonstrated above by increasing the resolution from T62 to T106. Currently mesoscale regional air quality models are often conducted at a resolution of 30–60 km to better simulate spatial distributions of ozone precursor concentrations and ozone production efficiency (e.g., Huang et al., 2007; Huang et al., 2008; Huang et al., submitted for publication). These regional models have produced a more realistic simulation of ozone diurnal cycle than our M_control and M_T106 (Huang et al., 2007). Running MOZART in such high spatial resolution, however, is difficult due to limitations in high-resolution meteorological fields and emissions. Nonetheless, the effects of ozone production efficiency can be demonstrated with the sensitivity experiment M_no2xoh, which produces 5–20 ppb lower D8hM ozone concentration than M_control over much of the U.S., thus reducing (increasing) the model biases over the eastern (western) U.S. (Fig. 5c,d, Table 2).

5. Conclusions and discussions

Using a modified version of MOZART-2.4, this study simulates the observed diurnal variation of surface ozone over the contiguous U.S. in summer 1999 and examines the impacts of different PBL mixing schemes, horizontal resolutions and emission inputs. The analysis focuses on five major regions: Northeast, Midwest, Southeast, California, and Southwest.

The diurnal variation of surface ozone concentration is greatly affected by the vertical mixing in the PBL. The strong mixing in the afternoon and weak mixing in the nighttime is critical for maintaining the diurnal pattern of surface ozone. With the default non-local mixing scheme capable of simulating both unstable and stable PBL, the control experiment captures very well the timing of the ozone diurnal cycle, with a phase shift of less than 1 h from observations for both the early morning minimum and the afternoon maximum. The biases are less than 5 ppb for the morning minimum, except over the Southeast. The difference between daily ozone maximum and minimum is overpredicted by 18.9 ppb over the Northeast and by 9.9 ppb over the Midwest, but is within 2 ppb of the observed over other regions. By comparison, the sensitivity experiments using a local mixing scheme significantly overpredict the amplitude of ozone diurnal cycle, with greater maximum and smaller minimum, since the PBL mixing is too weak during most of the day. On the other hand, assuming the PBL is fully mixed throughout the day substantially underestimates the ozone diurnal cycle, with greater nighttime concentrations but insignificant changes in the afternoon. Overall, the ozone maximum–minimum contrast is overpredicted by 10–34 ppb over the five regions by using the local mixing scheme; whereas it is underpredicted by 0–25 ppb, except over the Northeast, by assuming the fully mixed PBL.

The simulation of ozone diurnal cycle also depends on model horizontal resolution and emission inputs. As compared to the control experiment at the T62 resolution with the POET emissions, a resolution increase to T106 produces important differences in geographic distribution but insignificant changes in broad-area average over the five regions. However, using the less accurate emissions data of MOZ2 instead of POET, the amplitude of ozone diurnal cycle is more seriously overpredicted, with the ozone maximum–minimum contrast increasing from 18.9 ppb to 23.4 ppb over the Northeast and from 9.9 ppb to 12.7 ppb over the Midwest.

The model performance in simulating the daytime ozone is very different between the western and eastern U.S. The control simulation is quite realistic over the western U.S., where model biases in the D8hM ozone are

mostly less than 10 ppb. Over most of the eastern U.S., however, the model overestimates the D8hM ozone by about 5–25 ppb. This overprediction can be largely attributed to the enhanced ozone production efficiency resulting from the increased mixing of NO_x and VOC due to the coarse spatial resolution. Increasing the model resolution from T62 to T106 reduces the large D8hM ozone biases along the east coast from 44 ppb to 32 ppb, mainly due to the better representation of land–sea contrast.

This study has several important limitations. First, the use of the monthly mean emissions data precludes the assessment of the effects from diurnal and daily variations of precursor emissions. For a limited region like the U.S., one can incorporate high temporal variations of emissions as directly or scaled from the comprehensive dataset used in mesoscale regional air quality models (e.g., Huang et al., 2007; Huang et al., 2008; Huang et al., submitted for publication). One difficulty is the significant difference in the specification of VOC between the global and regional emission datasets. We are currently addressing this issue. In addition, precursor emissions in both POET and MOZ2 used here are representative of the late 1990s and not necessarily 1999. This may, in part, contribute to the large model biases over the eastern U.S. Second, the horizontal resolution used here (T62 and T106), albeit much higher than previous GCTM studies, is still too coarse to resolve the pollution variations in urban areas. As the resolution increases, the model is anticipated to more realistically simulate NO_x and VOC distributions and ozone production efficiency, and thus better resolve pollutant distributions at smaller scales. This may in part explain why the mesoscale regional air quality models significantly improve the ozone diurnal cycle simulation (Huang et al., 2007). Third, the model results also depend on the driving meteorological conditions. The currently available 6-hourly meteorological data are insufficient for resolving the diurnal variation. This may contribute to the overestimation of PBL mixing during the early evening under the non-local scheme. However, the exact effect cannot be determined without meteorological data at higher temporal resolution. Further research is required to address these issues and fully evaluate the impacts of various atmospheric and surface processes on ozone diurnal variations.

Despite these limitations, this study demonstrates the importance of the treatment of PBL mixing processes on the GCTM simulation of surface ozone diurnal cycle, consistent with the findings of Zhang et al. (2001) and Ku et al. (2001) for regional models. Incorporating the non-local mixing scheme, the modified MOZART-2.4 is capable of simulating the main features of the observed ozone diurnal variation at the regional scale, especially when using higher horizontal resolution ($\sim 1.1^\circ$) and updated precursor emissions. This increases its reliability when used alone for studying regional-scale pollutant distributions and changes (e.g., Lin et al., 2008a,b), or when providing lateral boundary conditions for chemicals to regional air quality models in studying pollution issues at smaller scales (e.g., Huang et al., 2008).

Acknowledgments

The research was supported in part by the United States Environmental Protection Agency Science to Achieve Results (STAR) Program under award number EPA RD-83337301-0 and the National Oceanic and Atmospheric Administration Education Partnership Program (EPP) COM Howard 631017. The authors acknowledge NCAR for the ECMWF ERA-40 data; GEIA/POET for the POET emission data; and NCSA/UIUC for the supercomputing support. We thank Peter Hess, Jean-Francois Lamarque and Larry Horowitz for discussions on the model performance and uncertainties. The views expressed are those of the authors and do not necessarily reflect those of the sponsoring agencies and other organizations including the Illinois State Water Survey.

References

Andreae, M.O., Merlet, P., 2001. Emission of trace gases and aerosols from biomass burning. Global Biogeochemical Cycles 15, 955–966.

Appel, K.W., Gilliland, A.B., 2007. Effects of Vertical-Layer Structure and Boundary Conditions on CMAQ-v4.5 and v4.6 Model. The 5th Annual CMAS Conference Chapel Hill, NC, October 16–18.

Brasseur, G.P., Hauglustaine, D.A., Walters, S., Rasch, P.J., Müller, J.-F., Granier, C., Tie, X.X., 1998. MOZART, a global chemical transport model for ozone and related chemical tracers: 1. Model description. Journal of Geophysical Research 103, 28,265–28,289.

Chen, X., Hulbert, D., Shepson, P.B., 1998. Measurement of the organic nitrate yield from OH reaction with isoprene. Journal of Geophysical Research 103, 25,563–25,568.

Chuong, B., Stevens, P.S., 2002. Measurements of the kinetics of the OH-initiated oxidation of isoprene. Journal of Geophysical Research 107 (D13), 4162. doi:10.1029/2001JD000865.

Fiore, A.M., Jacob, D.J., Bey, I., Yantosca, R.M., Field, B.D., Fusco, A.C., 2002. Background ozone over the United States in summer: origin, trend, and contribution to pollution episodes. Journal of Geophysical Research 107 (D15). doi:10.1029/2001JD000982.

Fiore, A., Horowitz, L.W., Purves, D.W., Levy II, H., Evans, M.J., Wang, Y., Li, Q., Yantosca, R.M., 2005. Evaluating the contribution of changes in isoprene emissions to surface ozone trends over the eastern United States. Journal of Geophysical Research 110, D12303. doi:10.1029/2004JD005485.

Granier, C., Guenther, A., Lamarque, J.F., Mieville, A., Muller, J.F., Olivier, J., Orlando, J., Peters, J., Petron, G., Tyndall, G., Wallens, S., 2005. POET, a database of surface emissions of ozone precursors. Available from: http://www.aero.jussieu.fr/projet/ACCENT/POET.php.

Guenther, A., Hewitt, C.N., Erickson, D., Fall, R., Geron, C., Graedel, T., Harley, P., Klinger, L., Lerdau, M., McKay, W.A., Pierce, T., Scholes, B., Steinbrecher, R., Tallamraju, R., Taylor, J., Zimmerman, P., 1995. A global model of natural volatile organic compound emissions. Journal of Geophysical Research 100, 8873–8892.

Hao, W.M., Liu, M.H., 1994. Spatial and temporal distribution of tropical biomass burning. Global Biogeochemical Cycles 8, 495–503.

Holtslag, A., Boville, B., 1993. Local versus nonlocal boundary-layer diffusion in a global climate model. Journal of Climate 6, 1825–1842.

Hong, S.-Y., Pan, H.-L., 1996. Nonlocal boundary layer vertical diffusion in a medium-range forecast model. Monthly Weather Review 124, 2322–2339.

Horowitz, L.J., Walters, S., Mauzerall, D.L., Emmons, L.K., Rasch, P.J., Granier, C., Tie, X., Lamarque, J.-F., Schultz, M.G., Tyndall, G.S., Orlando, J.J., Brasseur, G.P., 2003. A global simulation of tropospheric ozone and related tracers: description and evaluation of MOZART, version 2. Journal of Geophysical Research 108 (D24), 4784. doi:10.1029/2002JD2853.

Horowitz, L.W., Fiore, A.M., Milly, G.P., Cohen, R.C., Perring, A., Wooldridge, P.J., Hess, P.G., Emmons, L.K., Lamarque, J.F., 2007. Observational constraints on the chemistry of isoprene nitrates over the eastern United States. Journal of Geophysical Research 112, D12S08. doi:10.1029/2006JD007747.

Huang, H.-C., Liang, X.-Z., Kunkel, K.E., Caughey, M., Williams, A., 2007. Seasonal simulation of tropospheric ozone over the midwestern and northeastern United States: an application of a coupled regional climate and air quality modeling system. Journal of Applied Meteorology and Climatology 46, 945–960.

Huang, H.-C., Lin, J.-T., Tao, Z., Choi, H., Patten, K., Kunkel, K.E., Xu, M., Zhu, J., Liang, X-Z., Williams, A., Caughey, M., Wuebbles, D.J., Wang, J.X.L., 2008. Impacts of long-range transport of global pollutants and

precursor gases on US air quality under future climatic conditions. Journal of Geophysical Research 113, D19307.
Huang, H.-C., Liang, X.-Z., Kunkel, K.E., Williams, A., Caughey, M., Tao, Z. Simulation of continental US air quality on climatic time scales under present-day conditions. Journal of Geophysical Research, submitted for publication.
IPCC, 2001. In: Houghton, J.T., Ding, Y., Griggs, D.J., Noguer, M., van der Linden, P.J., Dai, X., Maskell, K., Johnson, C.A. (Eds.), Climate Change 2001: The Scientific Basis. Contribution of Working Group I to the Third Assessment Report of the Intergovernmental Panel on Climate Change. Cambridge University Press, Cambridge, United Kingdom, NY, USA 881pp.
Ku, J.-Y., Mao, H., Zhang, K., Civerolo, K., Rao, S.T., Philbrick, C.R., Doddridge, B., Clark, R., 2001. Numerical investigation of the effects of boundary-layer evolution on the predictions of ozone and the efficacy of emission control options in the northeastern United States. Environmental Fluid Mechanics 1, 209–233.
von Kuhlmann, R., Lawrence, M.G., Pöschl, U., Crutzen, P.J., 2004. Sensitivities in global scale modeling of isoprene. Atmospheric Chemistry and Physics 4, 1–17.
Lamarque, J.-G., Hess, P.G., Emmons, L., Buga, L., Washington, W., Granier, C., 2005. Tropospheric ozone evolution between 1890 and 1990. Journal of Geophysical Research 110, D08304. doi:10.1029/2004JD005537.
Lefohn, A.S., Oltmans, S.J., Dann, T., Singh, H.B., 2001. Present-day variability of background ozone in the lower troposphere. Journal of Geophysical Research 106, 9945–9958.
Lin, J.-T., Patten, K.O., Hayhoe, K., Liang, X.-Z., Wuebbles, D.J., 2008a. Effects of future climate and biogenic emissions changes on surface ozone over the United States and China. Journal of Applied Meteorology and Climatology 47 (7), 1888–1909. doi:10.1175/2007JAMC1681.1.
Lin, J.-T., Wuebbles, D.J., Liang, X.-Z., 2008b. Effects of intercontinental transport on surface ozone over the United States: present and future assessment with a global model. Geophysical Research Letters 35, L02805. doi:10.1029/2007GL031415.
Mellor, G.L., Yamada, T., 1982. Development of a turbulence closure model for geophysical fluid problems. Reviews of Geophysics and Space Physics 20, 851–875.
Mickley, L.J., Jacob, D.J., Field, B.D., 2004. Effects of future climate change on regional air pollution episodes in the United States. Geophysical Research Letters 31, L24103. doi:10.1029/2004GL021216.
Müller, J.-F., 1992. Geographical distribution and seasonal variation of surface emissions and deposition velocities of atmospheric trace gases. Journal of Geophysical Research 97, 3787–3804.
Müller, J.-F., Brasseur, G., 1995. IMAGES: a three-dimensional chemical transport model of the global troposphere. Journal of Geophysical Research 100, 16445–16490.
Murazaki, K., Hess, P., 2006. How does climate change contribute to surface ozone change over the United States? Journal of Geophysical Research 111, D05301. doi:10.1029/2005JD005873.
Olivier, J.G.J., Berdowski, J.J.M., Peters, J.A.H.W., Bakker, J., Visschedijk, A.J.H., Bloos, J.-P.J., 2001. Applications of EDGAR. Including a description of EDGAR 3.0: reference database with trend data for 1970–1995. RIVM, Bilthoven. RIVM report no. 773301 001/ NOP report no. 410200 051.
Padro, J., 1996. Summary of ozone dry deposition velocity measurements and model estimates over vineyard, cotton, grass and deciduous forest in summer. Atmospheric Environment 13, 2363–2369.
Seigneur, C., Pun, B., Pai, P., Louis, J.F., Solomon, P., Emery, C., Morris, R., Zahniser, M., Worsnop, D., Koutrakis, P., White, W., Tombach, I., 2000. Guidance for the performance evaluation of three-dimensional air quality modeling systems for particulate matter and visibility. Journal of the Air & Waste Management Association 50, 588–599.
Sillman, S., 1999. The relation between ozone, NO_x and hydrocarbons in urban and polluted rural environments. Atmospheric Environment 33, 1821–1845.
Sprengnether, M., Demerjian, K.L., Donahue, N.M., Anderson, J.G., 2002. Product analysis of the OH oxidation of isoprene and 1,3-butadiene in the presence of NO. Journal of Geophysical Research 107 (D15), 4268. doi:10.1029/2001JD000716.
Tarasick, D.W., Moran, M.D., Thompson, A.M., Carey-Smith, T., Rochon, Y., Bouchet, V.S., Gong, W., Makar, P.A., Stroud, C., Ménard, S., Crevier, L.-P., Cousineau, S., Pudykiewicz, J.A., Kallaur, A., Moffet, R., Ménard, R., Robichaud, A., Cooper, O.R., Oltmans, S.J., Witte, J.C., Forbes, G., Johnson, B.J., Merrill, J., Moody, J.L., Morris, G., Newchurch, M.J., Schmidlin, F.J., Joseph, E., 2007. Comparison of Canadian air quality forecast models with tropospheric ozone profile measurements above midlatitudes North America during the IONS/ICARTT campaign: evidence for stratospheric input. Journal of Geophysical Research 112, D12S22. doi:10.1029/2006JD007782.
Tie, X., Madronich, S., Walters, S., Edwards, D.P., Ginoux, P., Mahowald, N., Zhang, R.Y., Lou, C., Brasseur, G., 2005. Assessment of the global impact of aerosols on tropospheric oxidants. Journal of Geophysical Research 110, D03204. doi:10.1029/2004JD005359.
Troen, I., Mahrt, L., 1986. A simple model of the atmospheric boundary layer. Sensitivity to surface evaporation. Boundary Layer Meteorology 37, 129–148.
Uppala, S.M., Kållberg, P.W., Simmons, A.J., Andrae, U., da Costa Bechtold, V., Fiorino, M., Gibson, J.K., Haseler, J., Hernandez, A., Kelly, G.A., Li, X., Onogi, K., Saarinen, S., Sokka, N., Allan, R.P., Andersson, E., Arpe, K., Balmaseda, M.A., Beljaars, A.C.M., van de Berg, L., Bidlot, J., Bormann, N., Caires, S., Chevallier, F., Dethof, A., Dragosavac, M., Fisher, M., Fuentes, M., Hagemann, S., Hólm, E., Hoskins, B.J., Isaksen, L., Janssen, P.A.E.M., Jenne, R., McNally, A.P., Mahfouf, J.-F., Morcrette, J.-J., Rayner, N.A., Saunders, R.W., Simon, P., Sterl, A., Trenberth, K.E., Untch, A., Vasiljevic, D., Viterbo, P., Woollen, J., 2005. The ERA-40 re-analysis. Quarterly Journal of the Royal Meteorological Society 131, 2961–3012. doi:10.1256/qj.04.176.
U.S. EPA, 1999. Draft Guidance on the Use of Models and Other Analyses in Attainment Demonstrations for the 8-hour Ozone NAAQS EPA-454/R-99–004, May 1999.
U.S. EPA, 2001. Draft Guidance for Demonstrating Attainment of Air quality Goals for PM2.5 and Regional Haze. US Environmental Protection Agency, Research Triangle Park, NC.
Wei, C.-F., Kotamarthi, V.R., Ogunsola, O.J., Wuebbles, D.J., Avery, M.A., Blake, D.R., Browell, E.V., Sachse, G.W., Sandholm, S.T., 2002. Seasonal variability of ozone mixing ratios and budgets in the tropical southern Pacific: a GCTM perspective. Journal of Geophysical Research 107. doi:10.1029/2001JD000772.
Wesely, M.L., 1989. Parameterization of surface resistances to gaseous dry deposition in regional-scale numerical models. Atmospheric Environment 23, 1293–1304.
Wesely, M.L., Hicks, B.B., 2000. A review of the current status of knowledge on dry deposition. Atmospheric Environment 34, 2261–2282.
Wild, O., Prather, M., 2006. Global tropospheric ozone modeling: quantifying errors due to grid resolution. Journal of Geophysical Research 111, D11305. doi:10.1029/2005JD006605.
Wu, S.-L., Mickley, L.J., Jacob, D.J., Logan, J.A., Yantosca, R.M., Rind, D., 2007. Why are there large differences between models in global budgets of tropospheric ozone? Journal of Geophysical Research 112, D05302. doi:10.1029/2006JD007801.
Wuebbles, D.J., Patten, K.O., Johnson, M.T., Kotanarthi, R., 2001. New methodology for ozone depletion potentials of short-lived compounds: *n*-propyl bromide as an example. Journal of Geophysical Research 106, 14551–14572.
Wuebbles, D.J., Lei, H., Lin, J.-T., 2007. Intercontinental transport of aerosols and photochemical oxidants from Asia and consequences. Environmental Pollution 150, 65–84.
Yienger, J.J., Levy, II, H., 1995. Empirical model of global soil-biogenic NO_x emissions. Journal of Geophysical Research 100, 11447–11464.
Zhang, J., Rao, S.T., 1999. The role of vertical mixing in the temporal evolution of ground-level ozone concentrations. Journal of Applied Meteorology 38, 1674–1691.
Zhang, K., Mao, H., Civerolo, K., Berman, S., Ku, J.-Y., Rao, S.T., Doddridge, B., Philbrick, C.R., Clark, R., 2001. Numerical investigation of boundary-layer evolution and nocturnal low-level jets: local versus non-local PBL schemes. Environmental Fluid Mechanics 1, 171–208.
Zhang, L., Padro, J., Walmsley, J.L., 1996. A multi-layer model vs single-layer models and observed O_3 dry deposition velocities. Atmospheric Environment 30, 339–345.
Zhang, Y., Liu, P., Queen, A., Misenis, C., Pun, B., Seigneur, C., Wu, S.-Y., 2006a. A comprehensive performance evaluation of MM5-CMAQ for the summer 1999 southern oxidants study episode – part II: gas and aerosol predictions. Atmospheric Environment 40, 4839–4855.
Zhang, Y., Liu, P., Pun, B., Seigneur, C., 2006b. A comprehensive performance evaluation of MM5-CMAQ for the summer 1999 southern oxidants study episode – part III: diagnostic and mechanistic evaluations. Atmospheric Environment 40, 4856–4873.